



ELSEVIER

Physica A 300 (2001) 367–385

PHYSICA A

www.elsevier.com/locate/physa

# Two-parameter analysis of the scaling behavior at the onset of chaos: tricritical and pseudo-tricritical points

Alexander P. Kuznetsov<sup>a,b,\*</sup>, Sergey P. Kuznetsov<sup>a,b</sup>,  
Erik Mosekilde<sup>c</sup>, Ludmila V. Turukina<sup>a,b</sup>

<sup>a</sup>*Institute of Radio-Engineering & Electronics, Russian Academy of Sciences, Zelenaya 38, Saratov 410019, Russia*

<sup>b</sup>*Department of Nonlinear Processes, Saratov State University, Astrakhanskaya, 83, Saratov 410026, Russia*

<sup>c</sup>*Department of Physics, Technical University of Denmark, 2800 Kgs.Lyngby, Denmark*

Received 18 April 2001

---

## Abstract

We discuss the so-called tricritical points at the border of the period-doubling transition to chaos and examine to what extent the associated universality applies to 2D dissipative maps. As a concrete example, the Ikeda map is studied together with its 1D analog. For the approximate 1D map, the tricritical points appear as the terminal points of Feigenbaum's critical curves in the parameter plane. For the 2D map the same type of critical behavior does not occur in a rigorous sense. It may be observed as a kind of intermediate asymptotics, however, when one considers a finite number of period doublings. We refer to the associated points in the parameter plane as pseudo-tricritical. For the Ikeda map, we present estimates of the number of period doublings, after which the departure from the tricritical universality becomes essential. © 2001 Elsevier Science B.V. All rights reserved.

*PACS:* 05.45–a; 05.10.Cc; 05.70.Jk

*Keywords:* Iterative maps; Scaling; Bifurcation; Critical point

---

## 1. Introduction

Let us consider an invertible 2D map that describes the dynamics of some nonlinear dissipative system, e.g., a Poincaré map for a set of differential equations of the third

---

\* Corresponding author. Institute of Radio-Engineering & Electronics, Russian Academy of Sciences, Zelenaya 38, Saratov 410019, Russia.

*E-mail address:* alkuz@ns.sgu.ru (A.P. Kuznetsov).

order. Assume that the 2D map can approximately be reduced to some 1D map. Usually, this is possible in the case of sufficiently strong dissipation, i.e., when the Jacobian determinant for the original map is small, and the map is characterized by a strong compression of the phase area. Next, let us suppose that the transition to chaos in the system under study follows the Feigenbaum scenario. If the 1D map represents a good approximation, it will also display the Feigenbaum infinite cascade of period-doubling bifurcations. The bifurcation points, and the limit point of their accumulation (the critical point) for both maps will be close. Moreover, the constants of convergence for the bifurcation sequences in the 1D and 2D maps will be *exactly* the same; this is a consequence of the Feigenbaum universality.

If the system has two control parameters, then the period-doubling bifurcations occur along some curves in the parameter plane; these curves accumulate to a limit critical curve, in accordance with Feigenbaum's law. The Feigenbaum critical lines are present on the parameter plane of many 1D and 2D maps. For 1D maps, Chang et al. [1] have shown that the critical lines terminate at the so-called tricritical points. A specific feature of these points is that either the map itself, or the map defined for some number of iterations, has a quartic extremum rather than the usual quadratic one. For 1D maps the vicinity of a tricritical point in the parameter plane displays a special type of universal self-similar structure. This circumstance has been substantiated by means of the renormalization group (RG) approach [1]. Visually, the Feigenbaum critical line in the parameter plane looks like having a gap bounded from both sides by two tricritical points. This region, in turn, has a special fine organization. Here one can observe a set of cusp points with lines of folds (corresponding to saddle-node, or tangent, bifurcations), which emanate from the cusps. The period-doubling bifurcation curves run along the fold lines, and different curves go around the different cusps. These period-doubling curves also accumulate to some pieces of the Feigenbaum lines, and these pieces are terminated, in turn, at new tricritical points, and so on.

Much information about the details of this picture can be revealed by consideration of an elegant construction—the binary tree of superstable orbits, suggested, e.g., by MacKay and van Zeijts [2]. Let us depict on the parameter plane the paths corresponding to the existence of superstable orbits. It appears that these paths form a binary tree. Going up the branches of the tree, one arrives at the border of chaos, where specific scaling properties take place depending on the selected itinerary along the branches. The top of this tree organizes the complex structure of the parameter plane, and some particular set of branches gives rise to the set of tricritical points. Near the tricritical points a two-parameter scaling is observed, which is governed by the scaling factors

$$\delta_1 = 7.284686217 \dots, \quad \delta_2 = 2.8571241351 \dots \quad (1)$$

The accurate estimates for these factors follow from the RG analysis [1,2]. In fact, they appear as the eigenvalues for the RG equation linearized near the fixed point solution responsible for the tricritical behavior.

By virtue of the idea of universality, which is commonly believed to be an attribute of situations allowing the RG analysis, one could expect that the same universal pictures have to exist in the parameter planes for both the 1D and the 2D maps. It turns out, however, that with respect to the tricritical behavior, this is not the case. Indeed, it appears that the solution of the eigenvalue problem arising in the RG analysis of the tricritical situation yields, in addition to (1), one more relevant eigenvalue  $\delta_3 = -4.8294054153 \dots$  (see e.g. [3,4]). For 1D maps the corresponding perturbation of the RG equation solution appears to be excluded because of some sort of hidden symmetry. However, when the second dimension comes into play, this symmetry does not hold. The question is what the consequences of this circumstance are for the arrangement of the parameter plane of 2D dissipative maps. What happens with the tricritical universality? The aim of the present work is to discuss this question by appealing to a concrete example, the well-known Ikeda map and its 1D analog.

Using the relations between parameters of the original map and of the 1D analog one can approximately locate the points in the parameter plane, where the tricriticality should occur, if it was not destroyed. However, we develop a method to find the appropriate points with much higher accuracy. It is based on a search for the conditions of equality of multipliers (Floquet eigenvalues) for periodic orbits of sufficiently large periods  $N = 2^k$  and  $2N$ . This method yields the points that we call “*pseudo-tricritical*”. The disposition of the pseudo-tricritical points is in nice consistency with the complex fine structure of the parameter plane of the 2D map. On the other hand, there is a principal difference with the case of a 1D map. There we have an *infinite* number of levels of period doubling, moreover, the greater the level number, the better is the accuracy of the observed self-similarity for the parameter plane structure. In contrast, for 2D maps only a *finite* number of levels of approximate self-similarity under subsequent period doublings may be found near a pseudo-tricritical point. At sufficiently deep levels the picture becomes essentially different from the universal pattern characteristic for the 1D maps.

As we show, these circumstances are connected with the third eigenmode of the linearized RG equation. Moreover, we can give an estimate of the number of levels, for which a picture similar to that for the 1D map may be observed. Sometimes this number may be small, and sometimes remarkable large; it depends on the concrete pseudo-tricritical point selected for consideration. The detailed description of the changes in the small-scale arrangement of the parameter plane remains an unsolved problem and requires further investigations.

## 2. The Ikeda map and its one-dimensional approximation

The iterative map

$$z_{n+1} = A + Bz_n \exp(i(|z_n|^2 + \psi)) \quad (2)$$

was suggested by Ikeda et al. [5] to describe the dynamics of an optical ring cavity containing a medium with phase nonlinearity and driven by an external source of

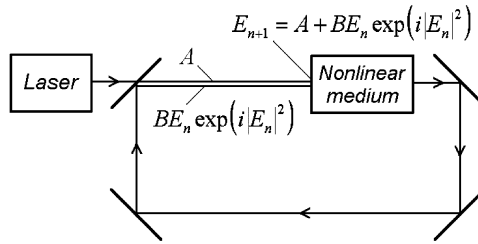


Fig. 1. Ikeda system—optical ring cavity with a nonlinear medium.  $E$  is a complex variable representing the amplitude and phase of the circulating electromagnetic wave.  $A$  represents the amplitude of the incident light, and  $B$  it the damping parameter.

intensive coherent radiation, a laser (Fig. 1). In (2),  $z$  is a complex dynamical variable representing the amplitude and phase of the electromagnetic wave circulating in the cavity,  $A$  is a parameter controlled by the intensity of the external source,  $B$  is the dissipation parameter, and  $\psi$  is a phase parameter accounting for a possible detuning of the cavity. In a certain approximation, the map (2) may also be derived as a stroboscopic map for a dissipative oscillator with cubic nonlinearity driven by periodic pulses [6–9]. In this last case,  $A$  has the sense of dimensionless amplitude of the pulses, and  $B$  is again the parameter of dissipation.

In Fig. 2, we present a chart of dynamical regimes for the Ikeda map (2) with vanishing phase parameter  $\psi$ . Regions of different periodic dynamics are shown in gray tones, and black color represents chaos. The areas of stability are bounded by lines of period-doubling bifurcations and by lines of tangent bifurcations, which look like folds emanating from the cusp points. The observed structure has been called a “crossroad area” [10]. In Fig. 2b we show the parameter plane chart for the larger Lyapunov exponent obtained with the technique suggested by several authors [11–13]. Here the gray tones designate different magnitudes of the Lyapunov exponent. For values from minus infinity to zero, the color varies from dark gray to white. Black areas correspond to positive values, i.e., to chaos. Such a coding helps to recognize the border between regular and chaotic dynamics. Note that the loci of parameter values corresponding to superstable cycles (the Lyapunov exponent tends to minus infinity) may be clearly seen, they are indicated by dark gray stripes. The cusp point vicinities look like “droplets” of light gray.

In the strongly dissipative case, the Ikeda map (2) allows reduction to a 1D map [8,9]. Let us suppose that the value of  $B$  is small and represent the variable  $z$  in the following form:

$$z = A(1 + B\tilde{z}) . \tag{3}$$

Substituting this expression into Eq. (2), we obtain the map:

$$\tilde{z}_{n+1} = (1 + B\tilde{z}_n) \exp \left( i \left( \varphi + \lambda \operatorname{Re} \tilde{z}_n + \frac{1}{2} \lambda B |\tilde{z}_n|^2 \right) \right) . \tag{4}$$

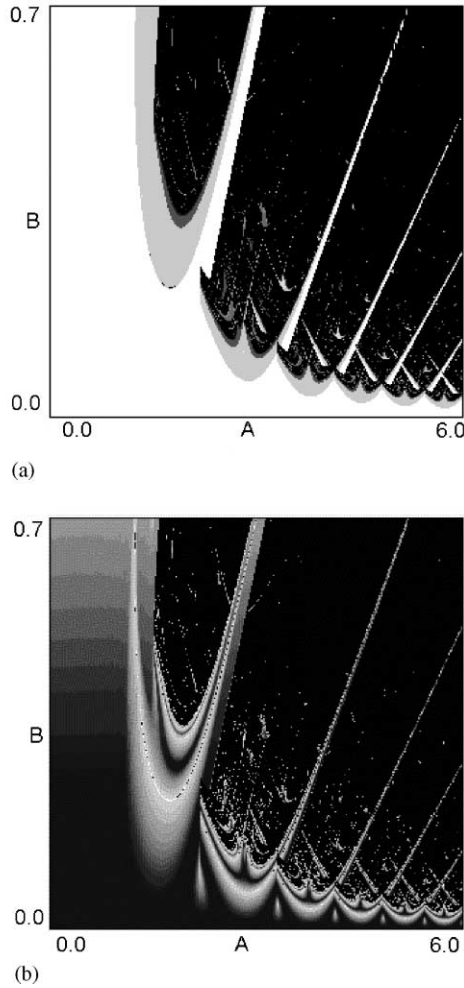


Fig. 2. Chart of dynamical regimes (a) and of the larger Lyapunov exponent (b) for the Ikeda map with  $\psi = 0$ .

It is convenient to introduce new parameters, namely,

$$\lambda = 2A^2B, \quad \varphi = A^2 + \psi. \tag{5}$$

As  $B$  is supposed to be small, we may neglect the terms containing this parameter in Eq. (4). Then for the real part  $\text{Re} \tilde{z}_n = \xi_n$  we obtain the 1D map:

$$\xi_{n+1} = \cos(\lambda \xi_n + \varphi). \tag{6}$$

By means of the variable change  $x = \lambda \xi + \varphi$  this map is finally transformed into a more convenient form, the cosine map

$$x_{n+1} = \lambda \cos x_n + \varphi. \tag{7}$$

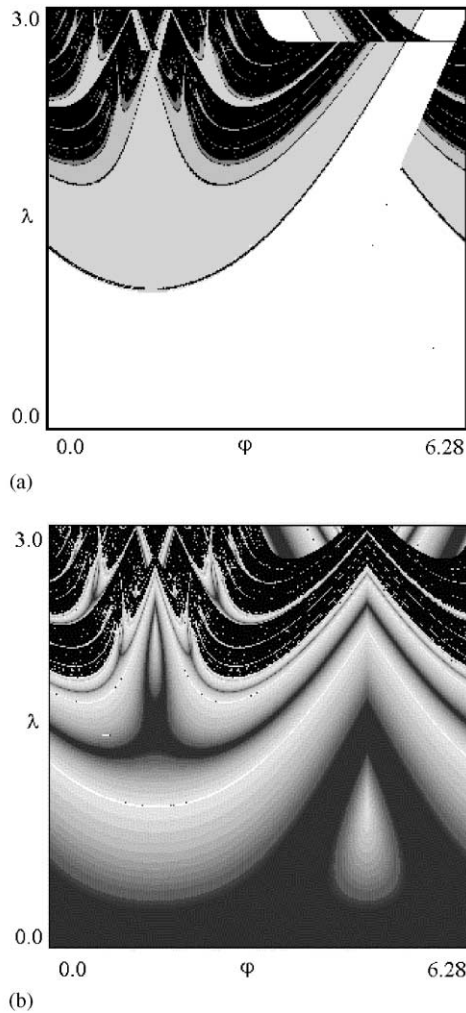


Fig. 3. Charts of dynamical regimes (a) and of the larger Lyapunov exponent (b) for the “cosine map”.

Fig. 3 presents charts of the dynamical regimes and the corresponding charts of the Lyapunov exponent for the 1D map (7). Objects are observed in the parameter plane analogous to those for 2D Ikeda map: the “crossroad areas”, cusp points, fold lines emanating from cusps, lines of period doubling, and regions of chaos. The correspondence between the charts of dynamical regimes for the Ikeda map and its 1D analog has been discussed in more detail in our previous publications [8,9]. Here we are going to concentrate on subtle details of the parameter plane arrangement associated with the tricritical points.

### 3. Tricritical points in the 1D map

To start, we would like to describe the procedure for accurately estimating the coordinates of the tricritical points for the 1D map. With this purpose, one can turn to a consideration of the binary tree of superstable orbits as proposed by MacKay and van Zeijts [2].

First, we note that at the particular parameter values  $\lambda = \pi/2$  and  $\varphi = \pi/2$  a period-2 orbit exists. This orbit passes both the minimum and the maximum of the map and is referred to as a doubly superstable cycle. Analogous cycles of other periods may exist at some exceptional points of the parameter plane  $(\lambda, \varphi)$ . We will refer to a doubly superstable cycle as a  $(p, q)$ -type of cycle if the maximum is mapped to the minimum after  $p$  iterations, and the minimum is mapped to the maximum after  $q$  iterations. Therefore, the period of such a cycle will be equal to  $p + q$ . Using this terminology, we say that the doubly superstable cycle at  $\lambda = \pi/2$  and  $\varphi = \pi/2$  is of type  $(1, 1)$ .

Starting at a superstable cycle of type  $(p, q)$  we may move on the parameter plane along one of two curves, one defined by the condition that the maximum is mapped to the minimum after  $p$  iterations, and the other defined by the condition that the minimum is mapped to the maximum after  $q$  iterations. Moving along such a path, we first observe a period-doubling bifurcation, and, after that, arrive at the point, where some new doubly-superstable cycle occurs. This cycle is of type  $(p, p + 2q)$  if we are on the first, and of type  $(2p + q, q)$  on the second curve. Starting at the new point of double superstability we can again choose one of two curves to follow, and so on. A set of all possible paths leading to the border of chaos via subsequent doubly superstable cycles gives rise to a tree-like graph on the parameter plane, the binary tree of superstable orbits [14–16]. This tree is depicted schematically in Fig. 4, and its real configuration on the parameter plane for the 1D cosine map is shown in Fig. 5. The types of doubly superstable cycles associated with the branching points of the tree are indicated in brackets.

One can use a two-symbol alphabet to code branches of the tree, say, by the binary digits 1 and 0. In this notation, each doubly superstable cycle will be represented by a finite string of the symbols. This code designates a unique route along the branches of the tree to the point on the parameter plane, where this cycle occurs. In Table 1 we give the parameter values  $\lambda, \varphi$  calculated numerically for doubly superstable cycles up to period 16. The types  $(p, q)$  of the doubly superstable cycles occurring on the road may be found step by step by application of the following rule defined subsequent symbols of the code:

$$\begin{aligned} \text{if symbol "1" then } p' &= p, \quad q' = 2q + p, \\ \text{if symbol "0" then } p' &= 2p + q, \quad q' = q. \end{aligned} \tag{8}$$

A path on the parameter plane associated with a given infinite code leads to a definite codimension-2 critical point at the border of chaos. There is a one-to-one correspondence between the set of codimension-2 critical points (the MacKay–van Zeijts critical

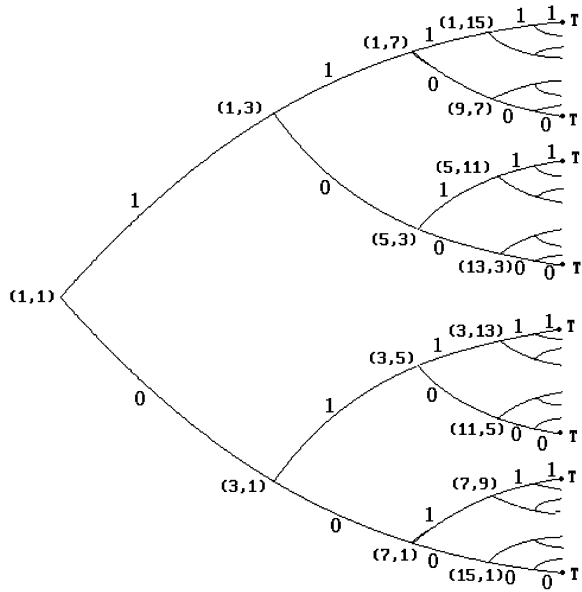


Fig. 4. Sketch of the binary tree of superstable orbits. Types of cycles are shown in brackets. The tricritical points (marked by letter T) are reached by following itineraries along the branches of the binary tree that end with an infinite tail of either 0's or 1's.

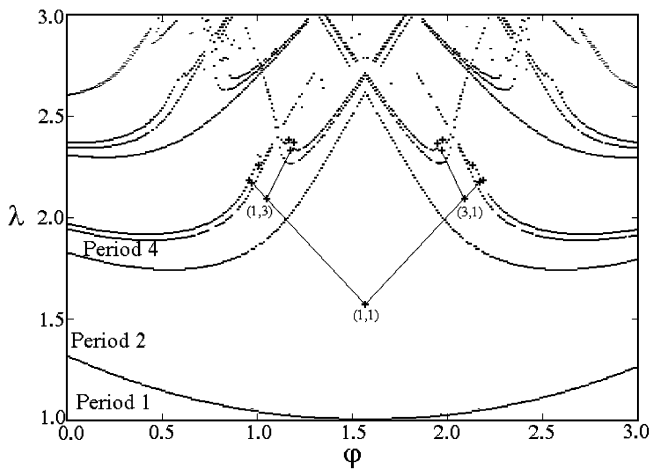


Fig. 5. Part of the parameter plane for the cosine map. The binary tree of superstable orbits is plotted according to data from Table 1.

points) and the set of infinite binary strings; this is an infinite set of continuum power. Tricritical points represent a special subset of the codimension-2 critical points.

To come to a tricritical point, we have to select a code containing an infinite tail of a particular repeating symbol, either 1 or 0. Note, that on the path along the branches

Table 1

Parameter values for the period 2–16 doubly superstable cycles from which the binary tree of superstable orbits for the “cosine map” are built

Code	Type	Period	$\varphi$	$\lambda$
	1,1	2	1.570796326795	1.570796326795
1	1,3	4	1.047197551197	2.094395102393
0	3,1	4	2.094395102393	2.094395102393
11	1,7	8	0.968186522936	2.173406130654
10	5,3	8	1.170649680989	2.333554082953
01	3,5	8	1.970942972601	2.333554082953
00	7,1	8	2.173406130654	2.173406130654
111	1,15	16	0.957291341158	2.184301312432
110	9,7	16	1.008414978327	2.258903333639
101	5,11	16	1.163683358739	2.384756302463
100	13,3	16	1.191333066393	2.369719516198
011	3,13	16	1.950259589657	2.369719516198
010	11,5	16	1.977909294851	2.384756302463
001	7,9	16	2.133177675262	2.258903333639
000	15,1	16	2.184301312432	2.184301312432

Table 2

Numerically calculated tricritical points of the “cosine map” corresponding to particular infinite codes

Code	Type	$\varphi$	$\lambda$
111111...	1, $q$	0.9555540392	2.1860386153
110000...	$p$ , 7	1.0160975436	2.2738881312
101111...	5, $q$	1.1622588937	2.3931674905
100000...	$p$ , 3	1.1947184432	2.3755653764
011111...	3, $q$	1.9468742103	2.3755653764
010000...	$p$ , 5	1.9793337599	2.3931674905
001111...	7, $q$	2.1254951100	2.2738881312
000000...	$p$ , 1	2.1860386115	2.1860386153

of the binary tree to a tricritical point one will meet, starting from some node, doubly superstable cycles of type  $(m, q)$  or  $(p, m)$ ; here  $m$  is constant while  $p$  and  $q$  tend to infinity (in such a way that  $m + q = 2^k$  or  $p + m = 2^k$ ). We say that the tricritical points are of types  $(m, \infty)$  or  $(\infty, m)$ , respectively. In Table 2, we present parameter values for tricritical points of the cosine map associated with some particular codes and Fig. 6 shows their location on the parameter plane. Figs. 5 and 6 correspond to the general picture, described in the Introduction. Namely, along the edges of the figures we observe accumulation of the period-doubling lines to the Feigenbaum critical curve, and in the central part of the pictures this line has a gap. Two main pieces of the critical line are terminated by tricritical points with codes 111111... and 000000..., respectively. The top of the binary tree enters into the region of the break (Fig. 5). The branches with codes like 100000..., 011111..., 010000..., 010000..., 101111..., 110000..., etc., give rise to other tricritical points, which terminate other pieces of the Feigenbaum

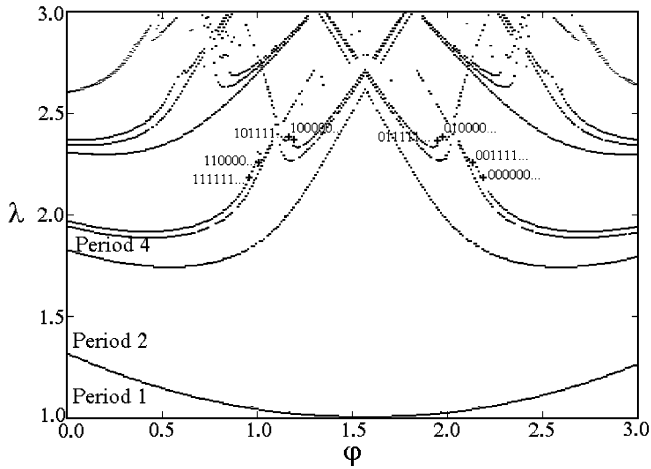


Fig. 6. Tricritical points for the cosine map. Coordinates of the points are calculated numerically and given in Table 2.

critical line. It is clear that the set of tricritical points appears as an essential attribute of the “crossroad area”. In fact, looking at the crossroad area configuration one can easily guess approximately where the tricritical points lie.

In a vicinity of each tricritical point, the 1D map demonstrates a universal organization of the parameter plane, and two-parameter scaling takes place. In accordance with the scaling law, the arrangement of a small part of the parameter plane near the tricritical point is reproduced under magnification by factors  $\delta_1 = 7.284686217$  along one axis and by  $\delta_2 = 2.8571241351$  along the other in a special, properly chosen coordinate system (see details in Refs. [1,17]).

Let us demonstrate the scaling properties for the attractor of the 1D map at a tricritical point. In Fig. 7 two attractors are shown, one corresponds to the tricritical point with code 111111..., and the other to 000000.... To observe scaling we choose a rectangle in a vicinity of the maximum of the map. Then we reproduce the picture under a number of steps of magnification by the factor  $\alpha = -1.69030297$  for the point of code 111111..., and by the factor  $\alpha^2 = 2.85712414$  for the point 000000... [1]. Observe the nicely repeating patterns on the diagrams relating to the subsequent levels.

#### 4. Pseudo-tricritical points in the Ikeda map

Now we turn to the two-dimensional Ikeda map. The expressions (5) determine the relation between parameters of the cosine map and the Ikeda map. As a rough approximation, we simply apply these formulas to reconstruct the binary tree from Fig. 5 and to depict it on the parameter plane of the 2D map. In fact, from this procedure we obtain not one, but a set of trees because of the periodicity of the cosine

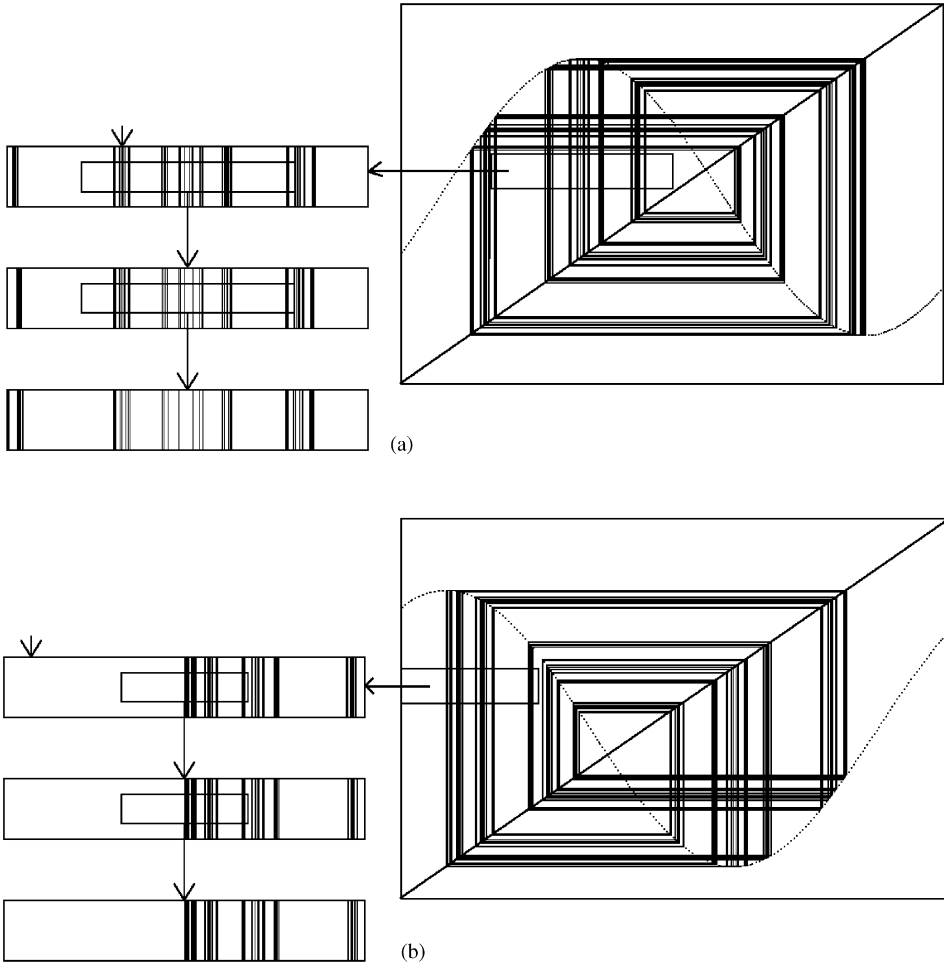


Fig. 7. “Portraits” of attractors at tricritical points with codes 111111... (a) and 000000... (b) for the cosine map. The scaling properties for these attractors are illustrated by fragments of the structure under subsequent magnification.

function (see Fig. 8). Now one can correlate the topography of the parameter plane for the Ikeda map (Fig. 2a) and the configuration of binary trees obtained from the 1D approximation. It may be seen that the 1D map provides an acceptable explanation of the general organization of the parameter plane for the Ikeda map.

Now let us turn to a more detailed comparison of the maps and consider the binary tree, which is the second from the left in Fig. 8. Table 3 gives the coordinates to the points for the Ikeda map in this area of the parameter plane as obtained by application of the relations (5) to the tricritical points of the 1D map. Disposition of these points in the parameter plane of the Ikeda map is shown in Fig. 9. On one hand, we can see that the picture is similar to that in Fig. 5. On the other hand, it seems that some of

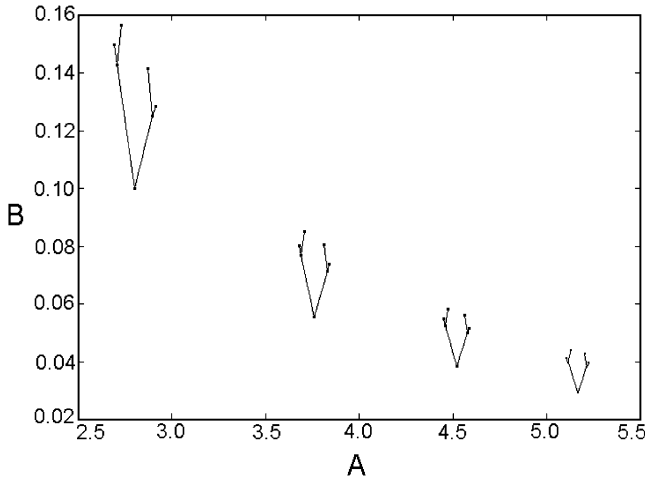


Fig. 8. Configuration of binary trees for the Ikeda map in the parameter plane. Coordinates of points corresponding to the doubly superstable cycles of the cosine map are calculated by using the coordinate transformation (5).

Table 3

Coordinates of the points, which correspond to the tricritical points of the “cosine map”, for Ikeda map. Points are calculated by using the parameter transformation (5)

Code	Type	<i>A</i>	<i>B</i>
111111 ...	1, <i>q</i>	2.6904905399	0.1509958096
110000 ...	<i>p</i> , 7	2.7017184995	0.1557610643
101111 ...	5, <i>q</i>	2.7286341273	0.1607135468
100000 ...	<i>p</i> , 3	2.7345756070	0.1588389912
011111 ...	3, <i>q</i>	2.8688080482	0.1443224889
010000 ...	<i>p</i> , 5	2.8744597870	0.1448206940
001111 ...	7, <i>q</i>	2.8997724768	0.1352107595
000000 ...	<i>p</i> , 1	2.9101931074	0.1290577883

the images of tricritical points are displaced towards the region of chaos, and some of them into the region of periodical behavior. This circumstance reflects the approximate nature of the 1D map used to find the tricritical points.

As we have mentioned in the introduction, formally speaking, the critical behavior associated with the tricritical points does not survive after addition of the second dimension. Nevertheless, it is possible to find points on the parameter plane of the 2D map that are analogous to the tricritical points with much higher accuracy than obtained from the above 1D approximation. Hence, we will speak about pseudo-tricritical points of the 2D map.

To construct a procedure to determine the location of the pseudo-tricritical points we wish to have a representation of the 2D map as a continuation by means of a smooth parameter change from the 1D map manifesting the tricritical behavior. Let us turn

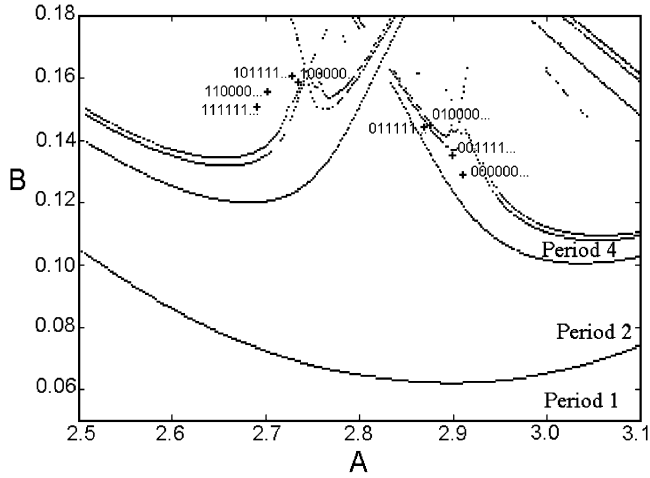


Fig. 9. Part of the parameter plane for the Ikeda map. Location of points that correspond to tricritical points of the cosine map is shown. Coordinates of these points are given in Table 3.

again to the form of the Ikeda map given by Eq. (4). We set there  $z = \xi + i\eta$  and, after separation of the real and imaginary parts, arrive to the equations

$$\begin{aligned} \xi_{n+1} &= (1 + B \cos \xi_n) \cos \left[ \lambda \xi_n + \varphi + \frac{1}{2} \lambda B (\xi_n^2 + \eta_n^2) \right] \\ &\quad - B \sin \xi_n \sin \left[ \lambda \xi_n + \varphi + \frac{1}{2} \lambda B (\xi_n^2 + \eta_n^2) \right], \\ \eta_{n+1} &= (1 + B \cos \xi_n) \sin \left[ \lambda \xi_n + \varphi + \frac{1}{2} \lambda B (\xi_n^2 + \eta_n^2) \right] \\ &\quad + B \sin \xi_n \cos \left[ \lambda \xi_n + \varphi + \frac{1}{2} \lambda B (\xi_n^2 + \eta_n^2) \right]. \end{aligned} \tag{9}$$

We recall that the new parameters  $\lambda$  and  $\varphi$  are expressed via the parameters of the original map by means of the relations  $\lambda = 2A^2B$  and  $\varphi = A^2 + \psi$  (5). If we formally set  $B = 0$  and regard  $\lambda$  and  $\varphi$  as independently controlled parameters, we come to a 1D mapping for the variable  $\xi$  defined by Eq. (6). As we have stated in the previous section, tricritical points are present in the parameter plane of the 1D map, which correspond to a particular case of the critical points of MacKay and van Zejits [2] (Table 2). Starting at  $B = 0$  from a certain tricritical point we may gradually increase  $B$  in Eq. (9) and adjust two other parameters to keep the larger multipliers for two cycles of sufficiently large periods  $N = 2^k$  and  $2N = 2^{k+1}$  equal to the universal constant  $\mu_C = -2.050940\dots$  (the asymptotic value of the multiplier characteristic for the tricritical point). Parameters  $A$  and  $\psi$  are expressed as

$$A = \sqrt{\lambda/2B}, \quad \psi = \varphi - A^2 = \varphi - \lambda/2B \tag{10}$$

and the procedure is continued up to the moment, when the difference  $\varphi - \lambda/2B$  will be equal to the desired value of  $\psi$  given for the original map. The values of  $A$  and  $B$  obtained in this way are regarded as coordinates of the pseudo-tricritical point for

Table 4  
Numerically found pseudo-tricritical points for the Ikeda map

Code	Type	<i>A</i>	<i>B</i>
111111...	1, <i>q</i>	2.7224102118	0.1498385065
110000...	<i>p</i> , 7	2.7294517267	0.1539308781
101111...	5, <i>q</i>	2.7544842490	0.1588737502
100000...	<i>p</i> , 3	2.7610044347	0.1570677015
011111...	3, <i>q</i>	2.8936523926	0.1436902000
010000...	<i>p</i> , 5	2.8988007984	0.1445571961
001111...	7, <i>q</i>	2.9237818787	0.1378390817
000000...	<i>p</i> , 1	2.9236246496	0.1379044458

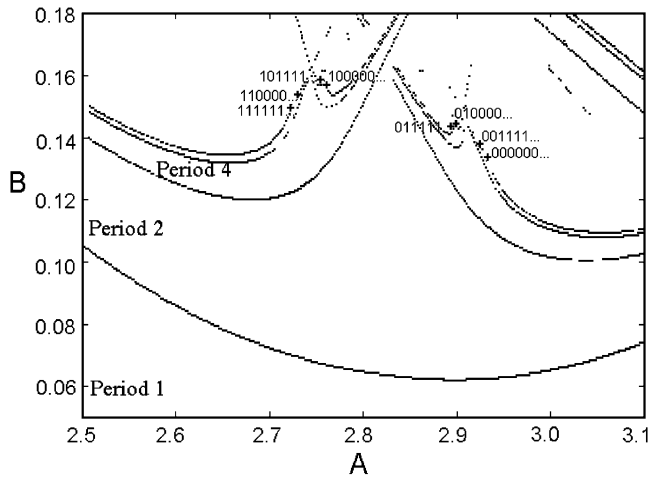


Fig. 10. Part of the parameter plane for the Ikeda map. Numerically calculated pseudo-tricritical points of the Ikeda map are shown. The coordinates of these points are given in Table 4.

the 2D-map, which are estimated on the level number *k*, i.e., via the cycles of period  $N = 2^k$  and  $2N = 2^{k+1}$ .

If the map actually exhibited tricriticality, the sequence of parameter values observed for increasing level number should converge to a definite limit, the tricritical point. For the 2D map this is not the case, and we observe another situation: the sequence initially looks like quickly converging (up to some finite, sometimes very deep level), but then it starts to diverge.

Coordinates of some pseudo-tricritical points of the Ikeda map, which relate to the tree selected for detailed analysis at  $\psi = 0$ , are given in Table 4. Geometrically, the locations of these points are shown in Fig. 10. Now one can compare two pictures, Figs. 6 and 10. Observe that the pseudo-tricritical points have come into proper position in the parameter plane; in respect to the parameter plane structure they are located precisely in the same manner as the tricritical points in the 1D map. Thus, the qualitative prediction of the parameter plane organization, which follows from analysis of

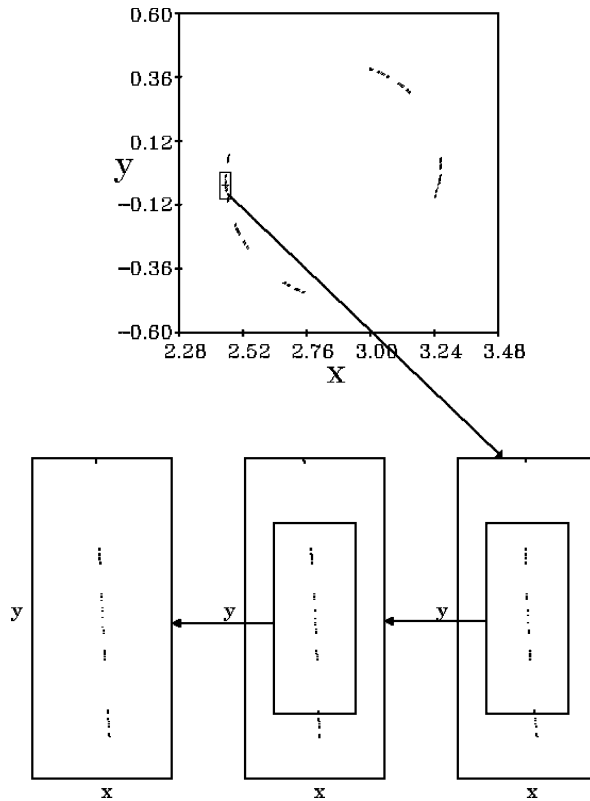


Fig. 11. “Portrait” of attractors at the pseudo-tricritical point with code 010000... for the Ikeda map. The lower part of the figure illustrates the scaling properties on this attractor.

the 1D map, works better and goes still further than the quantitative 1D approximation itself (compare the diagrams with Fig. 9).

Fig. 11 presents a “portrait” of the attractor at the pseudo-tricritical point with code 010000... for the Ikeda map. To illustrate the scaling property we take a fragment of the attractor and magnify it subsequently, step by step, with factor  $\alpha = -1.69030297\dots$ . Observe that self-similarity is manifested up to relatively high levels of resolution.

Now let us compare the Lyapunov charts in the vicinity of the tricritical point of the 1D map and for the corresponding pseudo-tricritical point of the 2D map (Fig. 12). Both diagrams are plotted in the plane  $(A, B)$ , and the critical points are located at the center of the pictures. Observe the rather good correspondence between the charts, which supports the impression of universality of the structure.

Nevertheless, the tricritical universality is not realized at deeper levels of resolution at the pseudo-tricritical points. Let us estimate the number of scaling levels, i.e., the number of period doublings that follow the scaling law. As we have noted, destruction of the tricritical universality is linked with the appearance of a third eigenmode in the

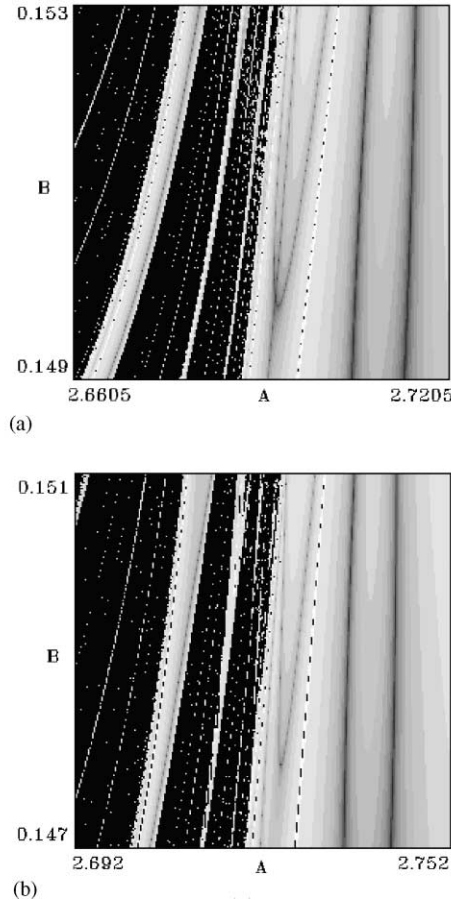


Fig. 12. Comparison of the charts of the Lyapunov exponent for the “cosine map” in the vicinity of a tricritical point (a) and for the Ikeda map in a vicinity of the corresponding pseudo-tricritical point (b). The tricritical and the pseudo-tricritical points are at the center of the picture.

solution of the RG equation with an eigenvalue  $\delta_3 = -4.8294054153\dots$ . Thus, we have to estimate the relative contribution of this “third mode”.

If we turn to a pseudo-tricritical point of types  $(1, \infty)$  or  $(\infty, 1)$ , the initial amplitude of the “third mode” is of order of the Jacobian of the 2D map, namely  $B^2$ . As the amplitude grows by a factor  $\delta_3$  for each period doubling, the amplitude will be of order  $B^2|\delta_3|^k$  after  $k$  doublings. This is also the order of the deviation for the larger multiplier from the universal value  $\mu_C$ . For pseudo-tricritical points of types  $(m, \infty)$  or  $(\infty, m)$ , i.e., for those codes that have repeating 1’s or 0’s as a tail after the first  $m$  alternating symbols, the  $m$ -fold iterated original map should be considered as the starting point for the “uniform” process of period doubling. The Jacobi determinant for the  $m$ -fold iterated map is  $B^{2m}$ . Thus, the deviation of the multipliers will behave as  $\Delta\mu \cong B^{2m}|\delta_3|^k$ . Let us take the deviation  $\Delta\mu$  of order 0.1 as a criterion for destruction

Table 5

Maximum number of period doublings at the pseudo-tricritical point of the 2D map

$m$	1	3	5	7
$k_{\max}$	1	5	10	15

of the tricritical scaling. Setting  $B^{2m}|\delta_3|^k \cong 0.1$  we readily obtain the estimate

$$k \cong \log(1/10B^{2m})/\log|\delta_3|. \quad (11)$$

Here  $k$  is the number of doublings counting from the first cycle of type  $(m, q)$  or  $(p, m)$  passed on the road to the given critical point along the binary tree.

For several concrete pseudo-tricritical points, the estimate of the number of doublings obeying the tricriticality scaling is given in Table 5. As we have found, the estimates are in good agreement with numerical calculations presented in Table 6. We list the values of  $A$  and  $B$  computed for the pseudo-tricritical points 011111... and 010000... from the condition of equality of multipliers for cycles of period  $N = 2^k$  and  $2N = 2^{k+1}$  together with the larger multiplier for the cycle of period  $4N$ . It may be seen that at some number of levels the period- $4N$  multiplier is approximately equal to the universal constant  $\mu_C = -2.050940\dots$ . However, at the levels of larger order it starts to deviate, alternating from step to step. Moreover, it is easy to check that the deviation grows approximately as  $\delta_3^k$ . This supports the assertion that the effect is linked with the “third mode” in the solution of the RG equation. (As we have checked, for 1D maps the similar computations do not show the phenomenon of growing multiplier deviation, but the observed value of the multiplier for the cycles of period  $4N$  tends to the universal constant  $\mu_C$ .)

## 5. Conclusion

In 1D non-invertible maps the tricritical points appear as terminal points of the Feigenbaum critical lines and represent one of important elements of the picture revealed by the two-parameter analysis of the transition to chaos via period doubling. The vicinity of each tricritical point is universally structured. There one can observe a set of cusp points with lines of tangent bifurcation emanating from them, “crossroad areas”, etc. We outline this important distinction of the tricritical behavior from the well-known one-parameter Feigenbaum universality. For the Feigenbaum universality, the correspondence between long-time behavior of 1D and 2D maps may be observed with high precision, as high as we wish; we simply have to choose a sufficiently large number of period-doubling. As to the tricriticality, for 2D-maps we can always find such a level of resolution of the subtle parameter plane or phase space structure that the universal self-similar structure is destroyed. Nevertheless, we are able to define for 2D invertible maps the points called “pseudo-tricritical”, which play in a sense an analogous role as the tricritical points for 1D maps. Near these points the same

Table 6  
Illustration of the destruction of the tricritical universality

Code	Type	Period $N$ and $2N$ cycles	Parameters $A$ and $B$	Multiplies of period- $4N$ cycle
011111 ...	3,q	4,8	$A = 2.893657906464569;$ $B = 0.1437049420044892$	-2.03269114169692
		8,16	$A = 2.89365379002949;$ $B = 0.1437003326788372$	-0.1962996596166289
		16,32	$A = 2.893652438822763;$ $B = 0.1436895223061902$	-2.064773677085535
		32,64	$A = 2.893652392631024;$ $B = 0.1436902000337308$	-2.054572492159918
		64,128	$A = 2.893652383949171;$ $B = 0.1436902646248461$	-1.992323194647993
		128,256	$A = 2.89365244208853;$ $B = 0.1436898988618876$	-2.329450019199727
010000 ...	p,5	4,8	$A = 2.899010063973471;$ $B = 0.144481320798527$	-2.387992241805486
		8,16	$A = 2.898821384713575;$ $B = 0.1445449084279817$	-2.235111782257143
		16,32	$A = 2.898791035946823;$ $B = 0.1445649163480796$	-1.854899286890886
		32,64	$A = 2.898801300018262;$ $B = 0.1445567741771848$	-2.082450162852802
		64,128	$A = 2.898800694444856;$ $B = 0.1445572862047433$	-2.034722626873405
		128,256	$A = 2.898800802028559;$ $B = 0.1445571929690272$	-2.053650327266563
		256,512	$A = 2.898800795714072;$ $B = 0.1445571984939539$	-2.047597028839509
		512,1024	$A = 2.898800798435668;$ $B = 0.1445571961036591$	-2.061466117994199

universal pictures are found as for the tricritical points, but this is true only on a finite number of levels of scaling. Thus, at the pseudo-tricritical points the universal behavior associated with the tricriticality appears only as a kind of intermediate asymptotics. We have examined a particular example of a 2D map, the Ikeda map, which allows for an approximate 1D description. As we have demonstrated, destruction of the tricritical

dynamics is due to the presence of a third relevant eigenvalue in the solution of the RG equation. At some pseudo-tricritical points the tricritical universality is valid for a surprisingly large number of period doublings. In such a case it may be impossible to distinguish the pseudo-tricritical behavior from true tricriticality in any realistic experiments. We suppose that our conclusions will be valid for a wide class of invertible dissipative 2D maps and for other multi-dimensional dissipative period-doubling systems.

## Acknowledgements

A.K., S.K., and L.T. acknowledge support from RFBR (grants 00-02-17509 and 01-02-06391) and from Research-Educational Center of Saratov University (grant of CRDF REC—006). S.K., and L.T. thank DTU for support of their visits to Denmark.

## References

- [1] S.J. Chang, M. Wortis, J.A. Wright, *Phys. Rev. A* 24 (1981) 2669.
- [2] R.S. MacKay, J.B.J. van Zeijts, *Nonlinearity* 1 (1988) 253.
- [3] S.P. Kuznetsov, *Phys. Lett. A* 169 (1992) 438.
- [4] A.P. Kuznetsov, S.P. Kuznetsov, I.R. Sataev, *Physica D* 109 (1997) 91.
- [5] K. Ikeda, H. Daido, O. Akimoto, *Phys. Rev. Lett.* 45 (1980) 709.
- [6] U. Parlitz, *Int. J. Bifurcation Chaos* 3 (1993) 703.
- [7] U. Parlitz, et al., *Int. Ser. Numer. Math.* 97 (1991) 283.
- [8] A.P. Kuznetsov, L.V. Turukina, *Proceedings of 2000 International Symposium on Nonlinear Theory and its Applications*, Vol. 2, 2000, p. 653.
- [9] A.P. Kuznetsov, L.V. Turukina, E. Mosekilde, *Int. J. Bifurcation Chaos* 11 (2001) 1065.
- [10] J. Carcasses, C. Mira, M. Bosch, C. Simo, J.C. Tatjer, *Int. J. Bifurcation Chaos* 1 (1991) 183.
- [11] J. Rössler, M. Kiwi, B. Hess, M. Marcus, *Phys. Rev. A* 39 (1989) 5954.
- [12] M. Marcus, B. Hess, *Comput. Graphics* 13 (1989) 553.
- [13] J.C. Bastos de Figueiredo, C.P. Malta, *Int. J. Bifurcation Chaos* 8 (1998) 281.
- [14] R.S. MacKay, C. Tresser, *Physica D* 27 (1987) 412.
- [15] R.S. MacKay, C. Tresser, *J. London Math. Soc.* 37 (1988) 164.
- [16] J.M. Gambaudo, J.E. Loss, C. Tresser, *Phys. Lett. A* 123 (1987) 60.
- [17] S. Fraser, R. Kapral, *Phys. Rev. A* 31 (1984) 1687.